Supplemental Methods

Supplemental Table

- **Supplemental Table 1: List of primers used for qRT-PCR.**

Supplemental Figures

- **Supplemental Figure 1: PLD4 expression also increases after CCl_4-induced liver fibrosis in mice.**
- **Supplemental Figure 2: Characterization of $PLD4^{-/-}$ mice.**
- **Supplemental Figure 3: $PLD4^{-/-}$ mice depict decreased expression of fibrotic markers at mRNA and protein levels than the $PLD4^{+/+}$ mice.**
- **Supplemental Figure 4: RNA sequencing identifies differentially expressed genes between the $PLD4^{+/+}$ and $PLD4^{-/-}$ mice.**
- **Supplemental Figure 5: $PLD4^{-/-}$ mice kidneys show differential expression of innate and adaptive immune components, decreased level of TGF-β signaling molecules and AAT as well as increased level of NE compared to the $PLD4^{+/+}$ mice.**
- **Supplemental Figure 6: PLD4-overexpressed HEK293T cells depict increased expression of AAT.**
- **Supplemental Figure 7. PLD4-mediated increased expression of TGF-β-induced fibrotic markers is decreased with NE treatment in HEK293T cells and primary human kidney fibroblasts co-culture system.**
- **Supplemental Figure 8: Treatment with PLD4 siRNA protects mice from kidney fibrosis.**

- **Supplemental Figure 9: Schematic illustration of the major steps involved in interaction proteomics.**
- **Supplemental Figure 10. Interaction network of the confirmed binding partners of PLD4 (CLGN, LMAN2 and SEL1L).**
- **Supplemental Figure 11. PLD4 inhibition down-regulates TrkA-mediated MAPK signaling pathway.**

SUPPLEMENTAL METHODS

Animals

Kidney fibrosis was induced in mice by two mechanistically different methods-(1) FA-induced and (2) UUO-induced kidney fibrosis. Mice were injected with a single dose of 250 mg/kg FA in 0.3 M sodium bicarbonate (vehicle), ip and sacrificed at days 1, 3, 7 and 14 post injection, and kidneys were collected. UUO in mice was performed under general anesthesia (50 mg/kg pentobarbital sodium, ip) by ligation of the left ureter as previously described.[1] Mice received lost fluid replacement (1 ml normal saline, sc, warmed at 37°C, immediately after surgery) as well as pain medication (buprenorphine, 0.05 mg/kg, sc, every 12 h for the first 2 days; 1st dose with the normal saline administered immediately after surgery and 3 additional doses in 50 µl normal saline). Mice were euthanized at days 3, 7 and 14 or 5 and 10 after UUO, and kidneys were collected.

In order to elucidate the role of proximal tubule specific PLD4 in kidney fibrogenesis, we bred the Cre and flox lines together for 2 generations and then selected breeders to produce the experimental genotypes PLD4$^{wt/wt}$Cre$^{+/-}$ mice (control group) and PLD4$^{fl/fl}$Cre$^{+/-}$ mice (proximal tubular cells-specific PLD4 knockout). For induction of the SLC34a1-driven Cre, mice were injected with 3 doses of 2mg tamoxifen (diluted in corn oil and 3% ethanol), every alternate day, *i.e.*, on day 1, 3 and 5 after FA injection. Mice were sacrificed on day 7 after FA injection (Figure 2D). Tamoxifen injections were started on day 1 after FA treatment, because our objective was to initiate PLD4 deletion after the induction of injury.

Liver fibrosis was induced in mice using carbon tetrachloride (CCl_4). CCl_4 (10% at 10 µl/g, ip) or its vehicle (corn oil) was administered twice a week for a total of 8 weeks. Mice were euthanized, and the liver was collected at 8 weeks post the initiation of CCl_4/vehicle injection.

In order to assess the therapeutic potential of PLD4 siRNA, kidney fibrosis was induced in mice by injecting 250 mg/kg FA or vehicle, ip and subsequently treated with PLD4 siRNA or

scrambled siRNA (30µg/200µl, iv) in RNAse-free phosphate-buffered saline (PBS) carriage medium at 2, 20, 38, 62 and 110 h after FA injection. Mice were sacrificed on day 7 after FA injection (Figure 4A). To assess injury markers, mice were sacrificed on day 2 after FA injection. Plasma creatinine was assessed by Isotope Dilution LC-MS MS at the O'Brien Core Center for Acute Kidney Injury Research (University of Alabama School of Medicine, Birmingham, Alabama, USA). Blood urea nitrogen (BUN) levels were measured in mice plasma using the Infinity Urea assay (Thermo Scientific) according to the manufacturer's instructions. KIM1 protein expression was assessed in mice kidneys using goat polyclonal anti-KIM1 antibody (R&D Systems, Inc., Minneapolis, MN).

De-identified human kidney tissue samples from patients with or without severe kidney fibrosis (n=10) were obtained from the Department of Pathology at Brigham and Women's Hospital. The Institutional Review Board approved the protocol for usage of paraffin embedded tissue sections from patients that underwent nephrectomy due to malignancies.

Western blot analysis

Western blot analysis was performed using standard protocols established in the laboratory.[2] Protein concentrations were determined using the BCA protein assay kit (Pierce, Thermo Scientific, MA), and equal amount of protein (25µg) was loaded and run on a polyacrylamide gel. The following primary antibodies were used for specific protein expression detection: rabbit polyclonal anti-PLD4 was purchased from MyBioSource, Inc., San Diego, CA. The antibody was raised against the immunogen sequence CLRQLFERDWSSRY, and the specificity was confirmed by running BLAST across different databases, lack of protein detection in the PLD4$^{-/-}$ mice at baseline and after fibrosis using Western blotting (Supplemental Figure 2D) as well as immunostaining (Supplemental Figure 2B), decrease of PLD4 expression in cells when transfected with PLD4 siRNA (Supplemental Figure 8A) and in

mice kidneys when injected with PLD4 siRNA (Figure 4B, Supplemental Figure 8C) and immunoprecipitation followed by immunoblotting using either anti-PLD4 antibody or anti-FLAG antibody (PLD4 plasmid was FLAG-tagged) (Figure 5E, Supplemental Figure 9B). Other primary antibodies used were rabbit polyclonal anti-fibronectin, mouse monoclonal anti-LMAN2, goat polyclonal anti-SEL1L and rabbit monoclonal anti-TrkA (Abcam, Cambridge, MA), mouse monoclonal anti-CLGN, rabbit polyclonal anti-collagen 1α1 and mouse monoclonal anti-FRS2α (Novus Biologicals, Littleton, CO), mouse monoclonal anti-α-SMA (Sigma-Aldrich, St. Louis, MO), rabbit polyclonal anti-AAT and rabbit polyclonal anti-NE (Proteintech Group, Inc., Rosemont, IL), rabbit polyclonal anti-Smad2, rabbit polyclonal anti-pSmad2, rabbit polyclonal anti-Smad3, rabbit polyclonal anti-pSmad3, rabbit polyclonal anti-ERK, rabbit polyclonal anti-pERK (Cell Signaling Technology, Beverly, MA), goat polyclonal anti-KIM1 (R&D Systems, Inc., Minneapolis, MN) and rabbit polyclonal anti-GAPDH (Abcam, Cambridge, MA). Horseradish peroxidase–conjugated secondary antibodies against rabbit (Cell Signaling Technology, Beverly, MA), mouse (Cell Signaling Technology, Beverly, MA) and goat (Abcam, Cambridge, MA) were used to detect the appropriate primary antibody. Bands were detected using enhanced chemiluminescence and captured with Gel Doc™ XR+ System (Bio-Rad, Hercules, CA). The blots were quantified with the help of Image Lab 4.1 software (Bio-Rad, Hercules, CA) and normalized with GAPDH expression.

Quantitative real-time PCR

Total RNA from kidney tissue was isolated using TRIzol (Invitrogen, Grand Island, NY) according to manufacturer's protocol and reverse transcribed to cDNA using the QuantiTect Reverse Transcription Kit (Qiagen, Valencia, CA). Quantitative RT-PCR was performed using a QuantiFast SYBR Green PCR Kit (Qiagen, Valencia, CA) on a LifeTechnologies QuantStudio 7 RT-PCR instrument (LifeTechnologies, Carlsbad, CA) as previously described.[3]

GAPDH was used as an endogenous control for normalization. Primer pairs used are listed in Supplemental Table 1.

Histology

Mouse organs were formalin-fixed, dehydrated in 70% etahnol, paraffin-embedded, sectioned and H&E stained at the Dana-Farber/Harvard Cancer Center Pathology Core Facilities. Mouse kidneys were stained with Picrosirius Red or Masson's Trichrome, and liver was stained with Picrosirius Red to assess the collagen deposition. Immunofluorescence staining was performed as described previously.[4] Mouse kidneys were fixed in 4% paraformaldehyde and transferred to sucrose solution (30%) for cryoprotection following which the kidneys were frozen in Tissue-Tek O.C.T. (VWR, Radnor, PA). Five μm thick kidney sections were permeabilized, blocked and labeled with primary antibodies, including rabbit anti-PLD4 (MyBioSource, Inc., San Diego, CA), FITC-conjugated anti-αSMA (Sigma-Aldrich, St. Louis, MO), Fluorescein labeled LTL and Fluorescein labeled DBA (Vector Labs, Burlingame, CA), rabbit polyclonal anti-fibronectin (Abcam, Cambridge, MA) and rabbit polyclonal anti-collagen 1α1 (Novus Biologicals, Littleton, CO). Slides were subsequently stained with species-specific FITC- or Cy3-conjugated secondary antibodies (Jackson ImmunoResearch Laboratories, West Grove, PA) and mounted with 4,6-diamidino-2-phenylindole-containing ProLong Gold Anti-fade Mountant (Life Technologies, Grand Island, NY). The images were captured on a Carl Zeiss AxioImager.M2 using AxioVision SE64 software or on a Maeby Nikon A1R point scanning confocal with spectral detection and resonant scanner on an inverted Nikon Ti microscope. The images were analyzed through NIH ImageJ using a color threshold algorithm.

Cell culture and transfections

For PLD4 subcellular localization experiment, HeLa cells and HEK293 cells were fixed with 4% paraformaldehyde and 4% sucrose for 10 min, permeabilized with PBS 0.1% Triton X-100, blocked with PBS 1% BSA and incubated with rabbit polyclonal anti-PLD4 (MyBioSource, Inc., San Diego, CA), mouse monoclonal anti-calnexin (Novus Biologicals, Littleton, CO), mouse polyclonal anti-golga1 (Abnova, Walnut, CA) and mouse monoclonal anti-Tom20 (Santa Cruz Biotechnology, Dallas, TX) overnight at 4°C. Slides were subsequently stained with species specific FITC- or Cy3-conjugated secondary antibodies (Jackson ImmunoResearch Laboratories, West Grove, PA) and mounted with 4,6-diamidino-2-phenylindole (DAPI)-containing ProLong Gold Anti-fade Mountant (Life Technologies, Grand Island, NY). The images were captured on a Carl Zeiss AxioImager.M2 using AxioVision SE64 software.

For PLD4 over-expression experiments, HEK293T cells were transfected with either pCMV Myc (pCMV) or PLD4 (Myc-DDK-tagged)-Human PLD4 (pCMV-PLD4) plasmids (Origene Technologies, Rockville, MD) using Lipofectamine 2000 (Life Technologies, Grand Island, NY) according to manufacturer's specifications. The cells were harvested 48h post-transfection for Western blot analysis.

Since PLD4 is not endogenously expressed in fibroblasts, a co-culture system was established using the primary human kidney fibroblasts (purchased from Cell Biologics, Chicago, IL) and HEK293T cells (transfected with pCMV or pCMV-PLD4) in order to examine the effect of PLD4 on TGF-β-induced fibrotic markers. Further, the effect of NE on the expression of fibrotic markers was also assessed. The co-cultured cells were treated with TGF-β (10ng/ml) and/or NE (50nM) for 48h, and the cells were harvested to measure the fibrotic markers. In another set of the experiment, cells were treated with NE (50nM) for 6h after the 48h treatment with TGF-β (10ng/ml).

For PLD4 knock down experiments, mIMCD3 cells were transfected with 100nM scrambled or PLD4 siRNA (Dharmacon, Lafayette, CO) using siPORT NeoFX transfection reagent (Life Technologies, Grand Island, NY) following the manufacturers protocol. We tested the efficacy of 4 siRNAs and found one (target sequence: UCAUCGUGCCUGUGGGAAA) that resulted in a significant silencing of PLD4 *in vitro,* which was further selected for *in vivo* experiments. The cells were harvested 24h post-transfection for Western blot analysis. mIMCD3 cells were chosen for this experiment since these are mouse epithelial cells and the goal was to examine the effectiveness of siRNA when injected in mice *in vivo*.

SUPPLEMENTAL TABLE 1. List of primers used for qRT-PCR

Gene	Forward primer	Reverse primer
GAPDH	GAATACGGCTACAGCAACAGG	GGTCTGGGATGGAAATTGTG
PLD1	CTTTCGTTGACTGAAGGCTCA	GACGTGTTCACCCTGGTCTC
PLD2	TGAGTTTGCGGAAGCACTGT	GCATTGTTCTCCGCTGTTTC
PLD3	GGAGTTCTCTCATCCACGCA	CACTTTGACGCCTCGTTCAT
PLD4	ATTCTGGGTTGTGGATGGG	CAAGGTCTTGAGCCAGGTTG
αSMA	GTCCCAGACATCAGGGAGTAA	TCGGATACTTCAGCGTCAGGA
Fibronectin	ATGTGGACCCCTCCTGATAGT	GCCCAGTGATTTCAGCAAAGG
Collagen 1α1	TGACTGGAAGAGCGGAGAGT	GTTCGGGCTGATGTACCAGT
IFN-γ	GTCCTGAGACAATGAACGCT	AAAGAGATAATCTGGCTCTGC
IL-1β	ACCTGTCCTGTGTAATGAAAGACG	TGGGTATTGCTTGGGATC
IL-17	ACTACCTCAACCGTTCCACG	CTTCCCAGATCACAGAGGGA
IL-4	TCGGCATTTTGAACGAGGTC	GAAAAGCCCGAAAGAGTCTC
TNF-α	CGCTCTTCTGTCTACTGAACTT	GATGAGAGGGAGGCCATT
IL-6	CAAGAGACTTCCATCCAGTTGCC	CATTTCCACGATTTCCCAGAGAAC
IL-10	CAGCCTTGCAGAAAAGAGAG	GGAAGTGGGTGCAGTTATTG
IL-2	AGGAACCTGAAACTCCCCAG	GTCAAATCCAGAACATGCCG
IL-12	GTGTCTTAGCCAGTCCCGAA	TCATGATCGATGTCTTCAGCA
IL-23	TCCCTACTAGGACTCAGCCAACTC	ACTCAGGCTGGGCACTG
iNOS	CGTGAAGAAAACCCCTTGTG	GGAGCCATTTTGGTGACTCTT
Arg1	CAGAGGTCCAGAAGAATGGAAG	AGCATCCACCCAAATGACAC

SUPPLEMENTAL FIGURES

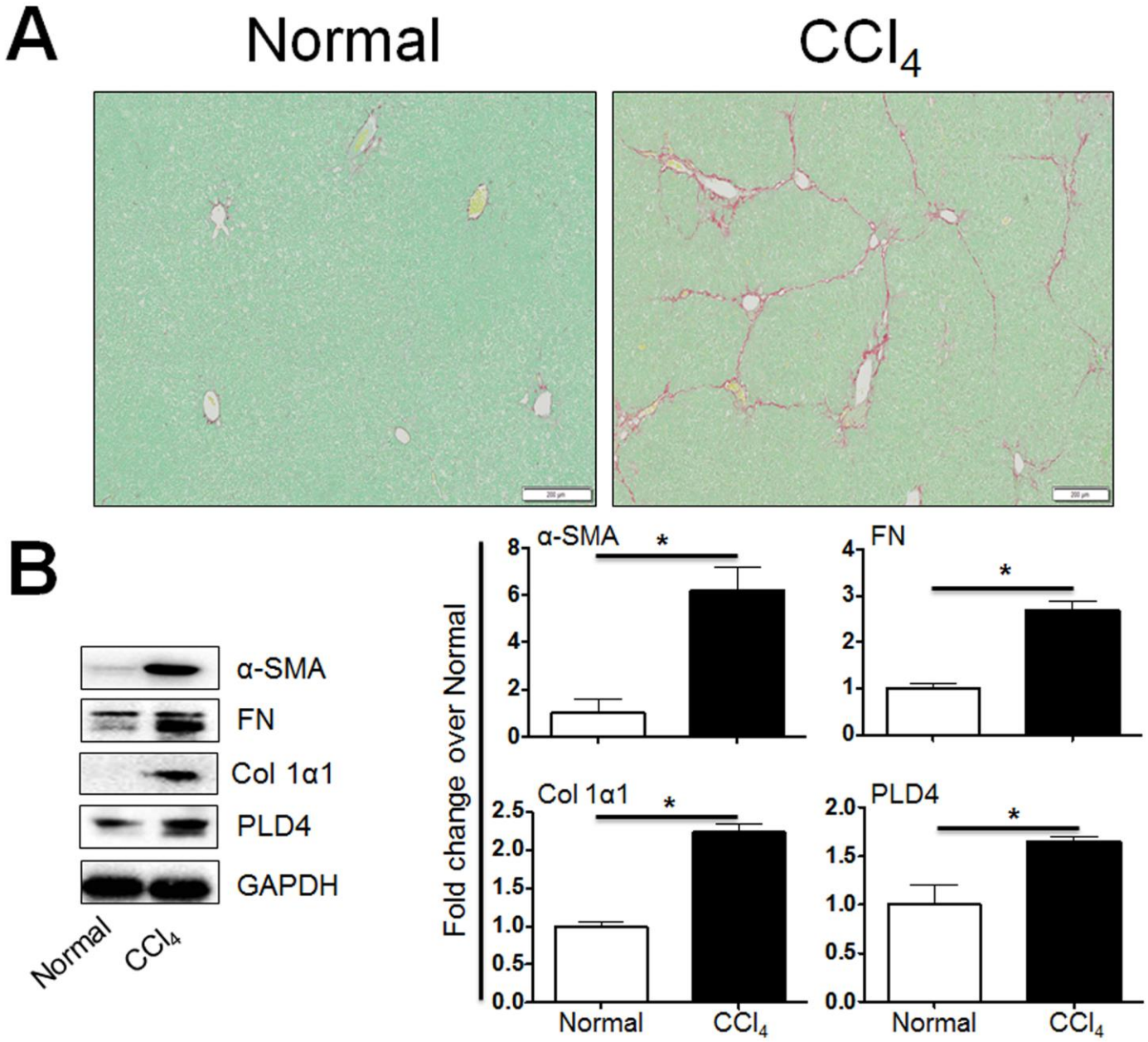

Supplemental Figure 1. PLD4 expression also increases after CCl_4-induced liver fibrosis in mice. (A) Representative photomicrographs of Picrosirius Red staining depicting collagen deposition in mice liver at baseline and following fibrosis. Scale bars, 200µm. (B) Protein expression of the fibrotic markers- α-SMA, fibronectin (FN) and collagen 1α1 (Col 1α1); and PLD4 in the liver of mice. Data were normalized to GAPDH and are presented as mean ± SEM (n = 4-10/group) of the fold change over Normal. *P<0.05.

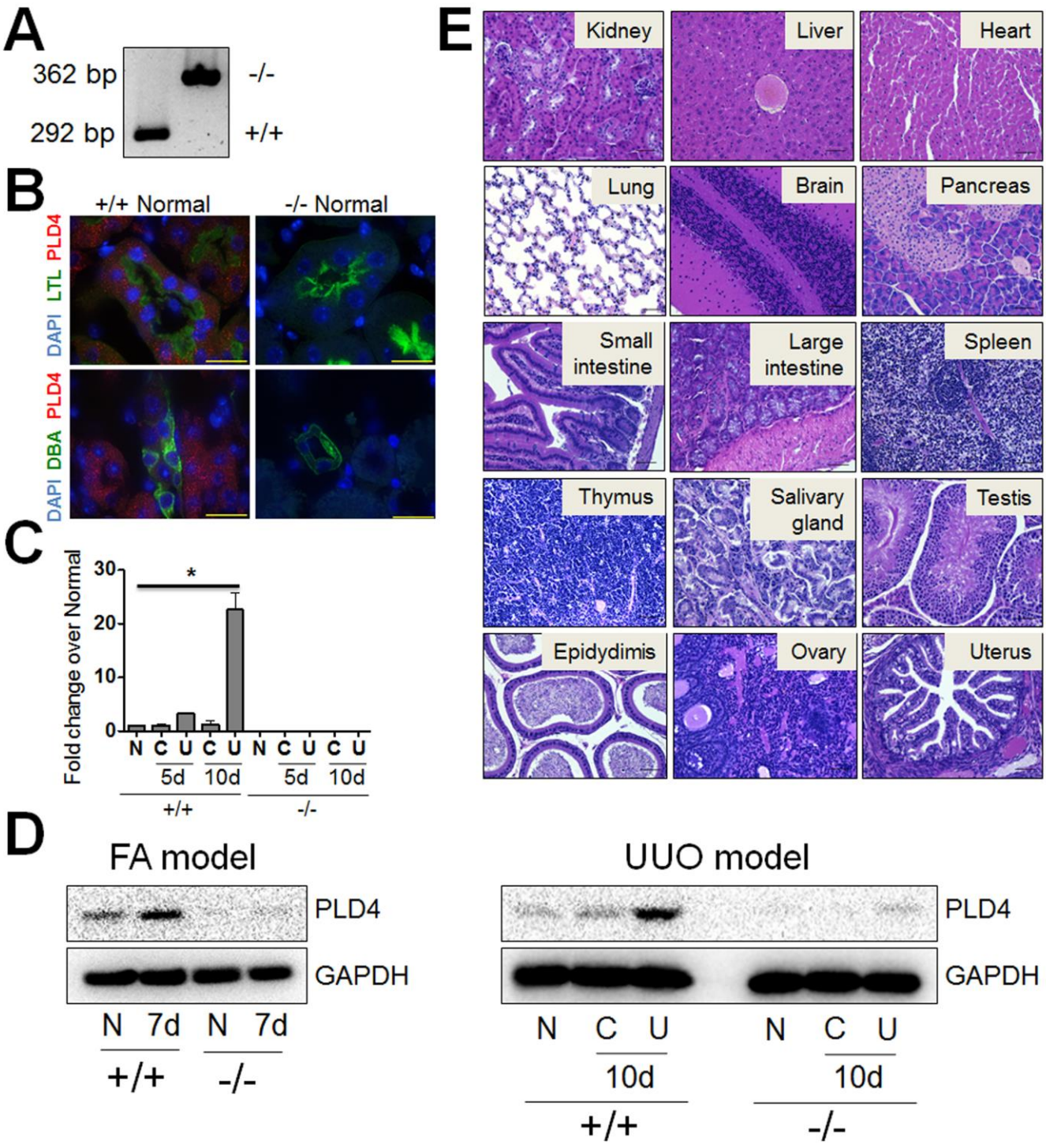

Supplemental Figure 2. Characterization of PLD4$^{-/-}$ mice. (A) Genotyping using PLD4 specific primers. (B) Co-staining of PLD4 with Lotus tetragonolobus Lectin (LTL, proximal tubule

marker) and Dolichos biflorus agglutinin (DBA, distal tubule marker) in $PLD4^{+/+}$ and $PLD4^{-/-}$ mice kidneys at baseline. Scale bars, 20µm. (C) qRT-PCR using PLD4 forward and reverse primers in $PLD4^{+/+}$ and $PLD4^{-/-}$ mice kidneys at baseline and following fibrosis. Data were normalized to GAPDH and are presented as mean ± SEM (n = 5/group) of the fold change over $PLD4^{+/+}$ Normal (N). *P<0.05. (D) Western blot analysis using anti-PLD4 antibody in the $PLD4^{+/+}$ and $PLD4^{-/-}$ mice at baseline and following fibrosis. (E) Representative images of histology after H&E staining of major organs in $PLD4^{-/-}$ mice at baseline (n = 5 males, 5 females). Scale bars, 50 µm. N-Normal, C-Contralateral, U-UUO.

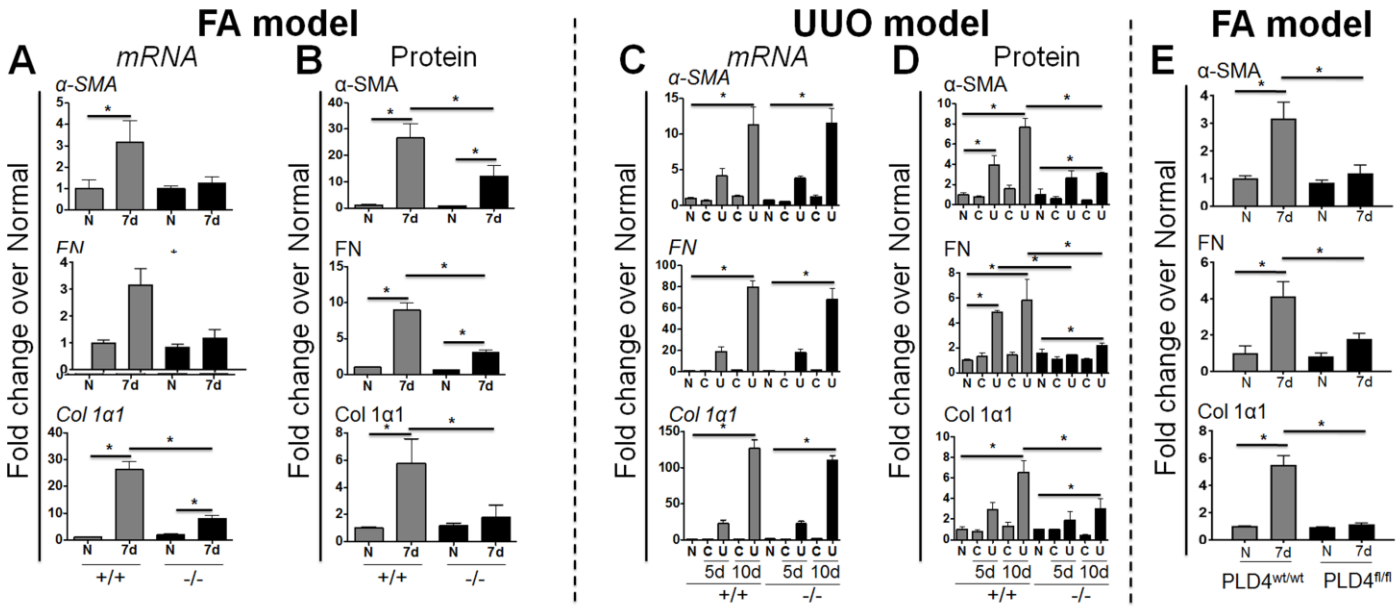

Supplemental Figure 3. PLD4$^{-/-}$ mice depict decreased expression of fibrotic markers at mRNA and protein levels than the PLD4$^{+/+}$ mice. Quantification of the fibrotic markers-α-SMA, fibronectin (FN) and collagen 1α1 (Col 1α1) at both (A, C) mRNA and (B, D) protein levels in the kidneys of mice treated with FA and subjected to UUO, respectively. Data were normalized to GAPDH and are presented as mean ± SEM (n = 5-7/group) of the fold change over PLD4$^{+/+}$ Normal (N). *P<0.05. N-Normal, C-Contralateral, U-UUO. (E) Quantification of the protein expression of α-SMA, fibronectin (FN) and collagen 1α1 (Col 1α1) in the kidneys of SLC34a1$^{GCE/+}$ PLD4 $^{wt/wt}$ and SLC34a1$^{GCE/+}$ PLD4 $^{fl/fl}$ mice treated with FA. Data were normalized to GAPDH and are presented as mean ± SEM (n = 5/group) of the fold change over Normal. *P<0.05.

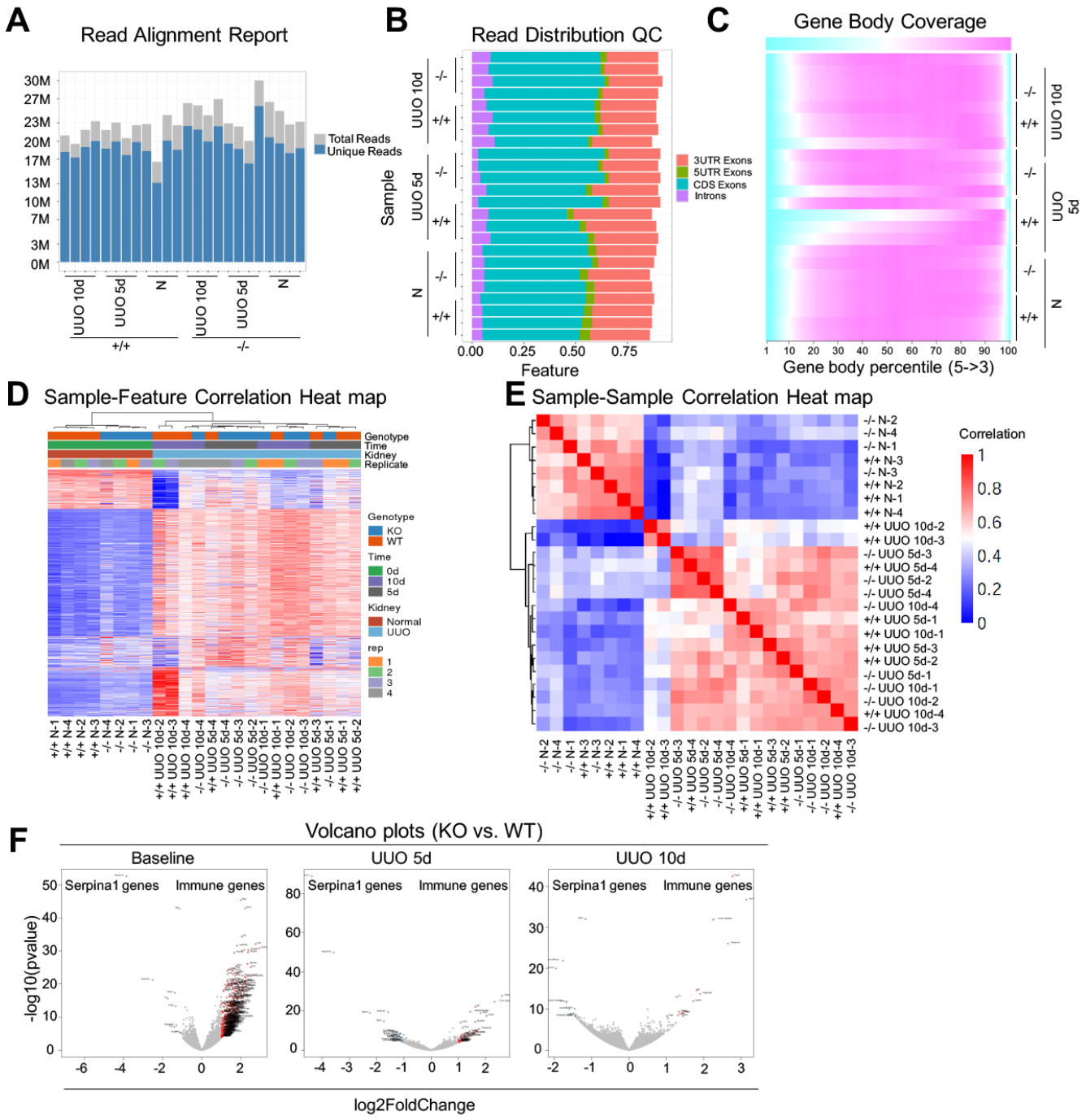

287

288

289 **Supplemental Figure 4.** RNA sequencing identifies differentially expressed genes between

290 the PLD4$^{+/+}$ and PLD4$^{-/-}$ mice. (A-D) RNA sequencing quality control. (E) Sample-sample

291 correlation heat map showing intra-group variation. (F) Volcano plots depicting the differentially

expressed immune (innate and adaptive) and serpina1 family genes between the PLD4$^{+/+}$ and PLD4$^{-/-}$ mice at baseline and following UUO (days 5 and 10) (n = 4/group).

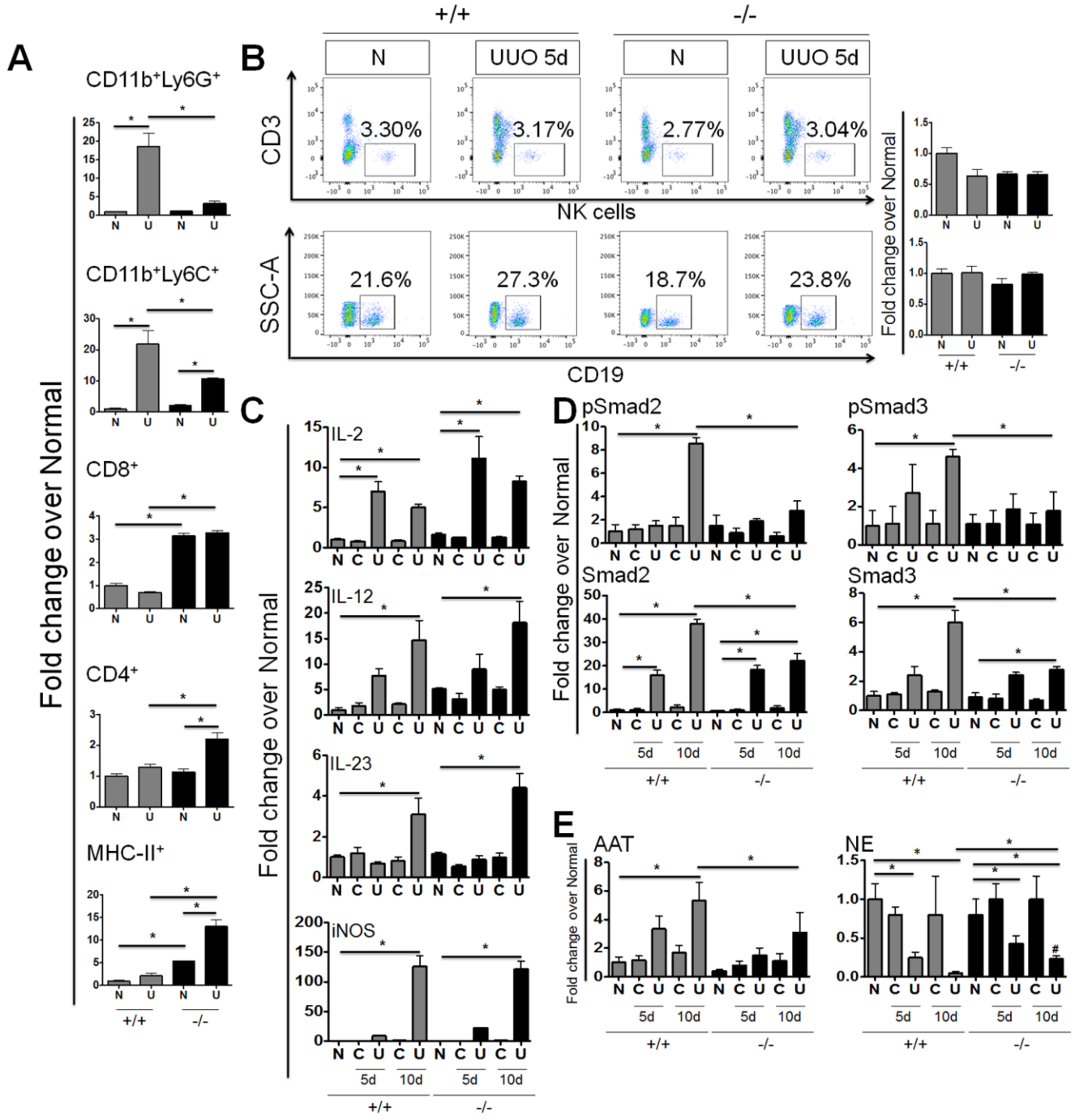

313

314

315 **Supplemental Figure 5.** PLD4$^{-/-}$ mice kidneys show differential expression of innate and

316 adaptive immune components, decreased level of TGF-β signaling molecules and AAT as well

317 as increased level of NE compared to the PLD4$^{+/+}$ mice. (A) Quantification of the levels of

$Cd11b^{+}Ly6G^{+}$, $Cd11b^{+}Ly6C^{+}$, $CD8^{+}$, $CD4^{+}$ and MHC-II^{+} cells in the kidneys of mice at baseline and following UUO (day 5) (n = 3/group). (B) Flow cytometric analysis of NK cells and B cells in the kidneys of mice at baseline and following UUO (day 5) (n = 3/group). (C) mRNA levels of cytokines in the kidneys of mice at baseline and following UUO (days 5 and 10) (n = 5-7/group). Quantification of the protein expression of (D) TGF-β signaling molecules, pSmad2, Smad2, pSmad3 and Smad3, and (E) AAT and NE in mice kidneys. Data were normalized to GAPDH and are presented as mean ± SEM (n = 5-7/group) of the fold change over $PLD4^{+/+}$ Normal (N). *P<0.05. N-Normal, C-Contralateral, U-UUO.

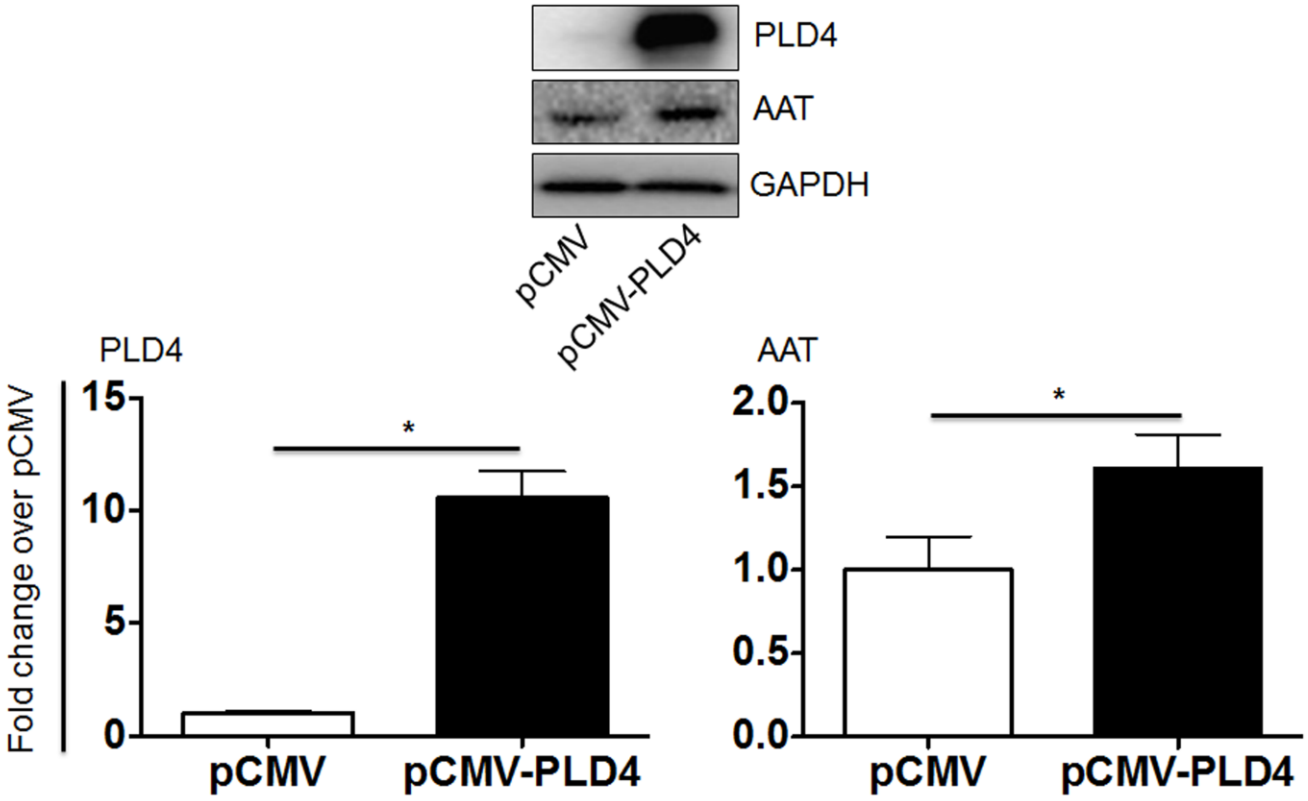

Supplemental Figure 6. PLD4-overexpressed HEK293T cells depict increased expression of AAT. Protein expression of PLD4 and AAT in HEK293T cells transfected with pCMV or pCMV-PLD4. Data were normalized to GAPDH and are presented as mean ± SEM (n = 9 wells from 3 independent experiments) of the fold change over pCMV. *P<0.05.

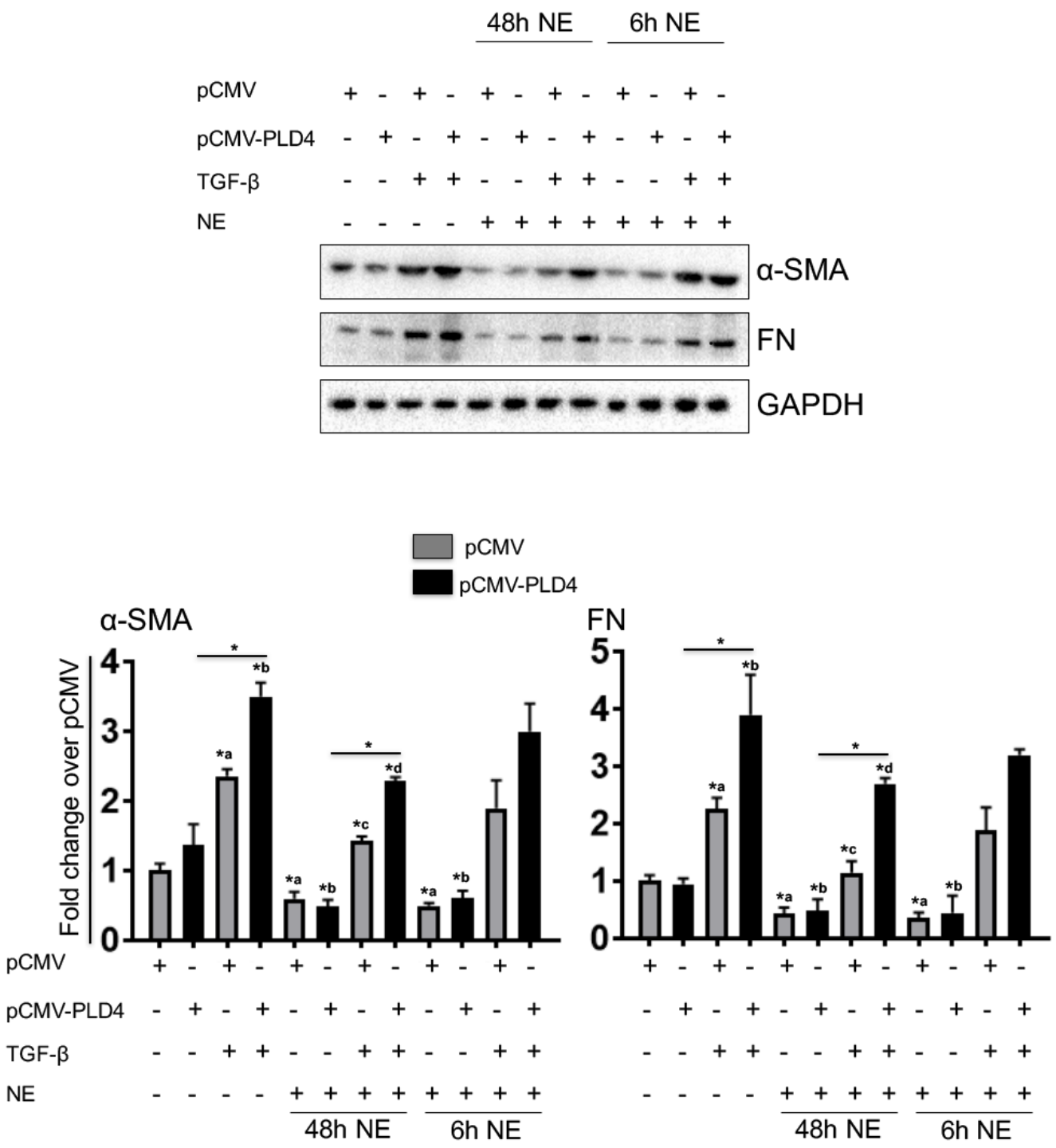

359

360 **Supplemental Figure 7.** PLD4-mediated increased expression of TGF-β-induced fibrotic
361 markers is decreased with NE treatment in HEK293T cells and primary human kidney
362 fibroblasts co-culture system. Protein expression of α-SMA and FN in primary human kidney
363 fibroblasts co-cultured with HEK293T cells (transfected with pCMV or pCMV-PLD4) treated

with TGF-β (10ng/ml, 48h) and/or NE (50nM, 48h along with TGF-β treatment or 6h after TGF-β treatment). Data were normalized to GAPDH and are presented as mean ± SEM (n=3 indicates 3 independent experiments with each experiment having treated and control samples in 3 wells/group) of the fold change over pCMV. *P<0.05, *[a] compared to pCMV, *[b] compared to pCMV-PLD4, *[c] compared to pCMV-TGF-β treatment, *[d] compared to pCMV-PLD4-TGF-β treatment.

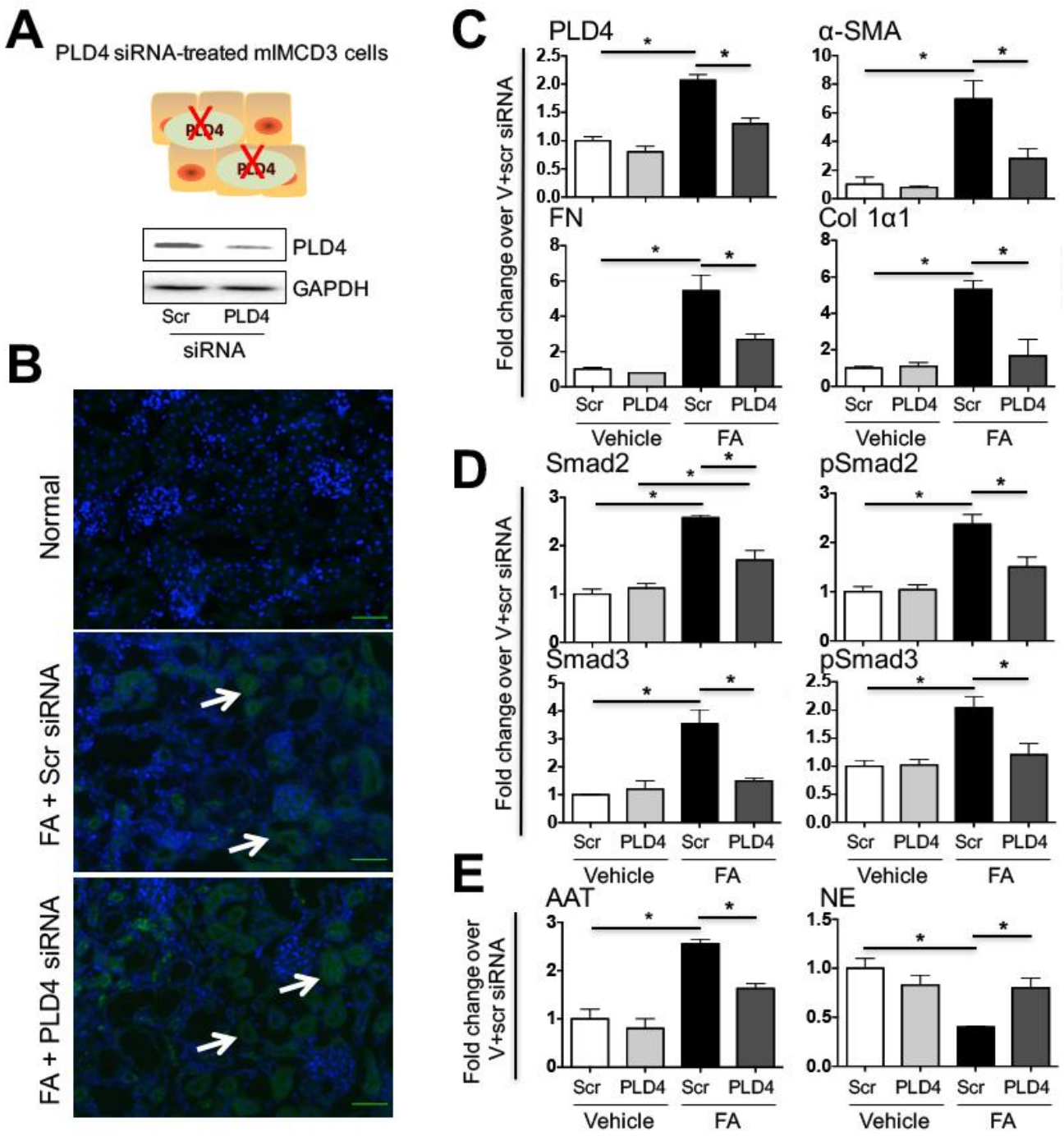

391

392 **Supplemental Figure 8.** Treatment with PLD4 siRNA protects mice from kidney fibrosis. (A)
393 PLD4 silencing in inner medullary collecting duct (mIMCD3) cells using siRNA. (B)
394 Photomicrographs depicting the delivery of siRNA (green, indicated with arrows) to the kidney
395 48h after the last dose of scrambled or PLD4 siRNA. (C) Quantification of the protein levels of
396 PLD4 and the fibrotic markers-α-SMA, fibronectin (FN) and collagen 1α1 (Col 1α1) in mice

kidneys. Quantification of the protein levels of (D) TGF-β signaling molecules, pSmad2, Smad2, pSmad3 and Smad3, and (E) AAT and NE in mice kidneys. Data were normalized to GAPDH and are presented as mean ± SEM (n = 5/group) of the fold change over Vehicle + scrambled siRNA. *P<0.05.

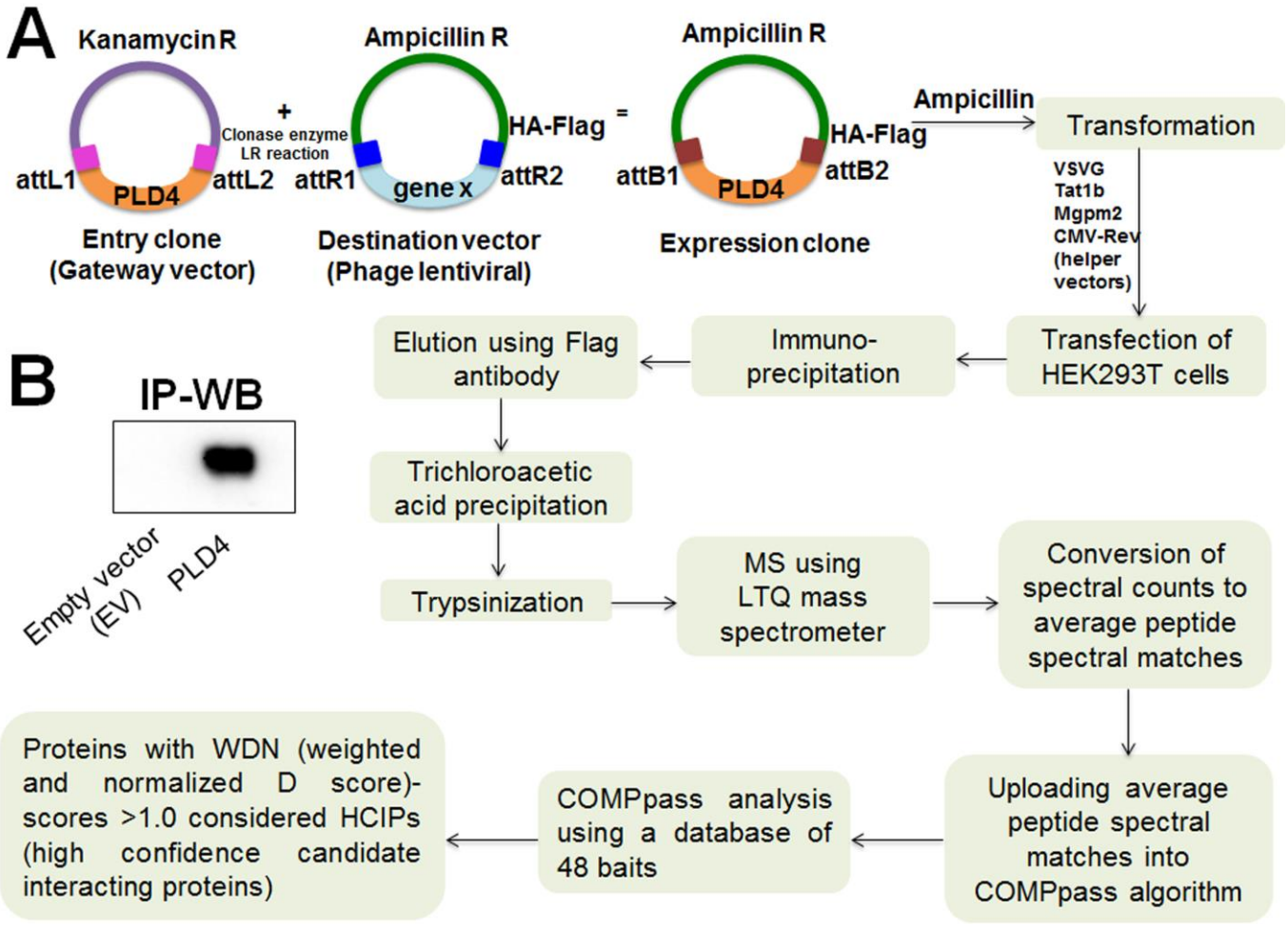

Supplemental Figure 9. Schematic illustration of the major steps involved in interaction proteomics. (A) Overview of the immunoprecipitation/mass spectrometry (IP/MS) methodology and (B) confirmation of the pull-down of PLD4 by Western blot.

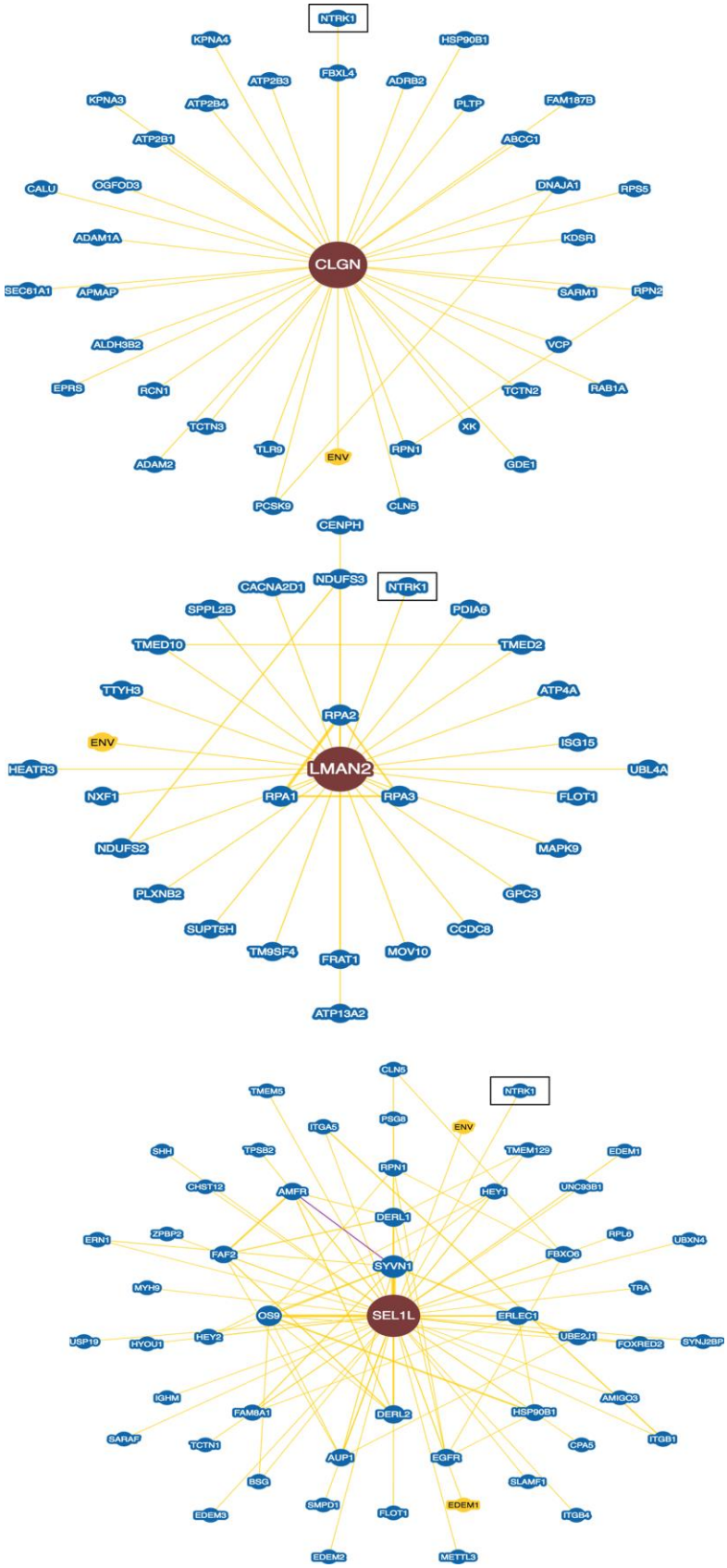
NTRK1
KPNA4
HSP90B1
FBXL4
ATP2B3
ADRB2
KPNA3
ATP2B4
PLTP
FAM187B
ATP2B1
ABCC1
CALU
OGFOD3
DNAJA1
RPS5
ADAM1A
KDSR
CLGN
SEC61A1
APMAP
SARM1
RPN2
ALDH3B2
VCP
EPRS
RCN1
TCTN2
RAB1A
TCTN3
XK
TLR9
ENV
RPN1
GDE1
ADAM2
PCSK9
CLN5
CENPH
CACNA2D1
NDUFS3
NTRK1
SPPL2B
PDIA6
TMED10
TMED2
TTYH3
ATP4A
RPA2
ENV
ISG15
HEATR3
LMAN2
UBL4A
NXF1
RPA1
RPA3
FLOT1
NDUFS2
MAPK9
PLXNB2
GPC3
SUPT5H
CCDC8
TM9SF4
FRAT1
MOV10
ATP13A2
CLN5
TMEM5
NTRK1
ITGA5
PSG8
ENV
SHH
TPSB2
TMEM129
EDEM1
RPN1
CHST12
AMFR
HEY1
UNC93B1
DERL1
ERN1
ZPBP2
RPL6
UBXN4
FAF2
FBXO6
SYVN1
MYH9
TRA
OS9
SEL1L
ERLEC1
USP19
HYOU1
HEY2
UBE2J1
FOXRED2
SYNJ2BP
IGHM
AMIGO3
FAM8A1
DERL2
HSP90B1
SARAF
TCTN1
CPA5
ITGB1
AUP1
EGFR
BSG
SLAMF1
SMPD1
FLOT1
EDEM1
EDEM3
ITGB4
EDEM2
METTL3

Supplemental Figure 10. Interaction network of the confirmed binding partners of PLD4 (CLGN, LMAN2 and SEL1L). The interaction network shows Neurotrophic Receptor Tyrosine Kinase 1 (NTRK1), also known as Tropomyosin-Related Kinase A (TrkA) as a common interactor of CLGN, LMAN2 and SEL1L (https://thebiogrid.org).

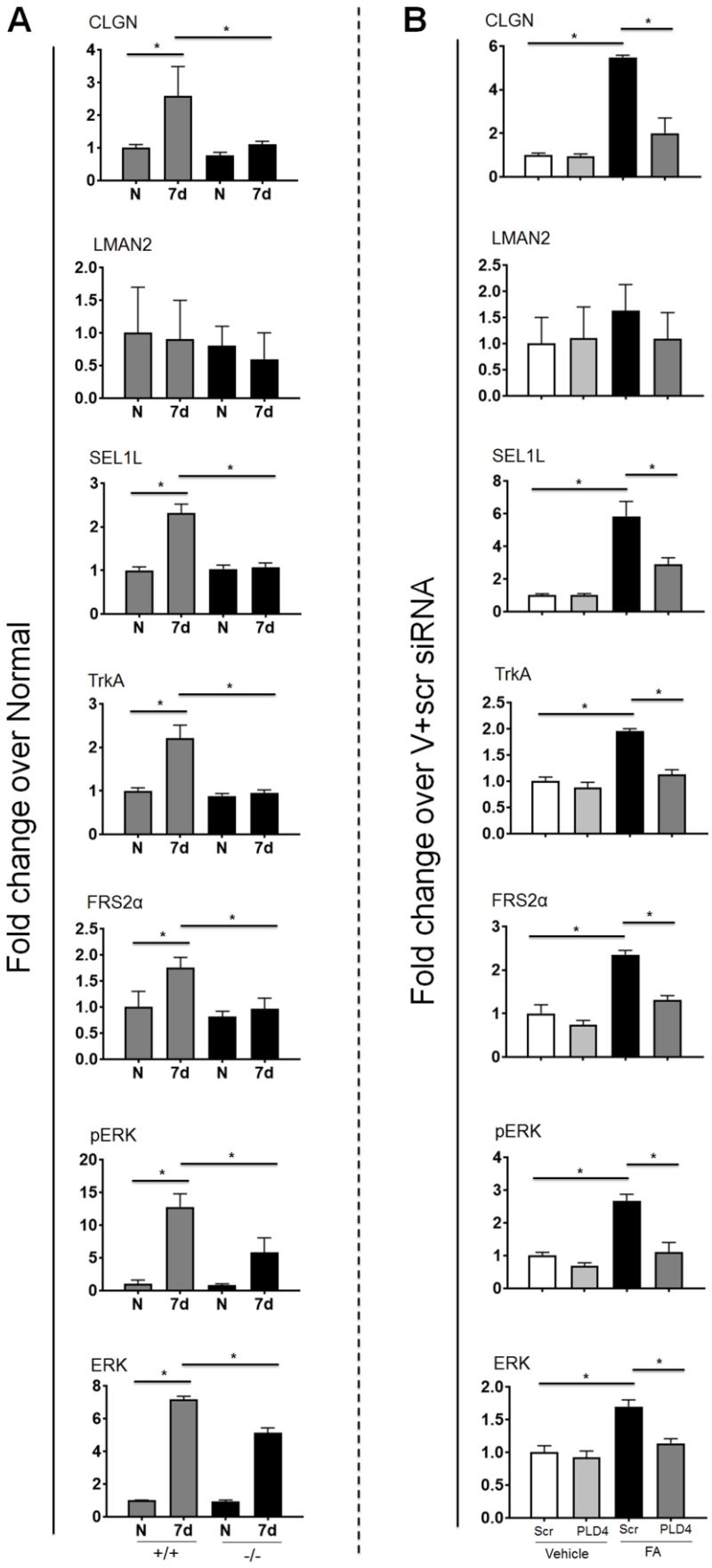
A
B
Fold change over Normal
Fold change over V+scr siRNA
CLGN
LMAN2
SEL1L
TrkA
FRS2α
pERK
ERK
N
7d
+/+
-/-
Scr
PLD4
Vehicle
FA

Supplemental Figure 11. PLD4 inhibition down-regulates TrkA-mediated MAPK signaling pathway. (A) Quantification of the protein levels of CLGN, LMAN2, SEL1L, TrkA, FRS2α, pERK and ERK in the kidneys of (A) $PLD4^{+/+}$ and $PLD4^{-/-}$ mice treated with FA and (B) mice treated with FA and/or siRNA (scr and/or PLD4). Data were normalized to GAPDH and are presented as mean ± SEM (n = 5/group) of the fold change over $PLD4^{+/+}$ Normal (N) and Vehicle + scrambled siRNA, respectively. *P<0.05.

REFERENCES

1. Craciun FL, Ajay AK, Hoffmann D, Saikumar J, Fabian SL, Bijol V, Humphreys BD, Vaidya VS: Pharmacological and genetic depletion of fibrinogen protects from kidney fibrosis. *Am J Physiol Renal Physiol* 307**:** F471-484, 2014

2. Ajay AK, Kim TM, Ramirez-Gonzalez V, Park PJ, Frank DA, Vaidya VS: A bioinformatics approach identifies signal transducer and activator of transcription-3 and checkpoint kinase 1 as upstream regulators of kidney injury molecule-1 after kidney injury. *J Am Soc Nephrol* 25**:** 105-118, 2014

3. Cardenas-Gonzalez M, Osorio-Yanez C, Gaspar-Ramirez O, Pavkovic M, Ochoa-Martinez A, Lopez-Ventura D, Medeiros M, Barbier OC, Perez-Maldonado IN, Sabbisetti VS, Bonventre JV, Vaidya VS: Environmental exposure to arsenic and chromium in children is associated with kidney injury molecule-1. *Environ Res* 150: 653-662, 2016

4. Jadhav S, Ajay AK, Trivedi P, Seematti J, Pellegrini K, Craciun F, Vaidya VS: RNA-binding Protein Musashi Homologue 1 Regulates Kidney Fibrosis by Translational Inhibition of p21 and Numb mRNA. *J Biol Chem* 291**:** 14085-14094, 2016